A01-34115

AIAA 2001-3330

Development of A Colloid Micro-Thruster For Flight Demonstration on the Emerald Nanosatellite

F. M. Pranajaya and M. A. Cappelli
Aeronautics and Astronautics Department
Mechanical Engineering Department
Stanford University
Stanford, CA

37th AIAA/ASME/SAE/ASEE
Joint Propulsion Conference and Exhibit
8-11 July 2001
Salt Lake City, Utah

AIAA-2001-3330 *AIAA Joint Propulsion Conference*

DEVELOPMENT OF A COLLOID MICRO-THRUSTER FOR FLIGHT DEMONSTRATION ON THE EMERALD NANOSATELLITE

FREDDY M. PRANAJAYA[1] AND MARK A. CAPPELLI[2]

A colloid thruster functions by electrostatically generating and accelerating sub-micron droplets of propellant to high velocities. The technology is attractive because of the weight and size of the integrated package, its high efficiency, low power consumption and inert propellant. The development of the thruster prototype at Stanford University is aimed for a proof-of-concept flight-testing on board a 20-kg university satellite. The thruster system incorporates a modular and expandable design that uses a software-programmable micro-controller to control the telemetry, propellant system, the high-voltage power systems, the operation of the thruster, as well as the interfacing with the satellite bus. The modularity of the system allows for testing of three thruster core designs. Single-emitter and multi-emitter arrays consisting 0.006 in OD / 0.002 in ID stainless-steel capillary needles were constructed and tested. The half-kilogram Colloid Micro Thruster (CMT) system measures 4 in by 4 in by 8 in, consumes 6 watts of total power, contains 10 ml of 2.0 M sodium-iodide/glycerol propellant, and is capable of producing up to 4 micronewton of thrust per needle emitter at up to 200 seconds specific impulse. The thruster system is being prepared for flight qualification for launch on a 2002 Space Shuttle mission.

I. INTRODUCTION

Space mission designers have long been relying on electric propulsion because of its high specific impulse, allowing higher total delta-V, which makes it suitable for long space missions or for spacecraft with limited fuel storage capacity. Despite this advantage, the high power consumption and specialized power supply requirements have made electric propulsion options unattractive for Class I (5-20 kg) and Class II (1-5 kg) spacecraft.

Colloid micro-thruster (CMT) technology is expected to satisfy the need for high-performance propulsion units for small spacecraft. In a recent review paper, Mueller [1] concluded: "... of all micro-electric primary propulsion options reviewed, colloid thrusters are quite possibly the most suited for microsatellite propulsion applications." Previous research has already demonstrated that colloid propulsion technology has significant potential, although it has not nearly reached the level of maturity in its development, as have other electric rocket technologies. It is also apparent from a review of the colloid rocket literature, that there is much work to be done on developing an understanding of the fundamental processes involved in the formation and acceleration of the electrospray, and in the characterizing of the emission process. Furthermore, there is little or no research on the on miniaturizing this technology so that it may be suitable for micro- and nanosatellite propulsion applications, and, equally important, on the integration of this technology for flight. Current as well as future research efforts are motivated primarily by the need from the micro- and nanosatellite community, and by the need for a high-performance, economical propulsion option for advanced missions utilizing a formation of multiple spacecraft.

II. BACKGROUND

A. Theory

The Colloid thruster works by the electrostatic atomization, charging, and acceleration of the propellant. The governing equations for the thrust, T, and specific impulse, I_{sp}, of the CMT can be derived from the rocket equations:

---

[1] Ph.D. Candidate, Department of Aeronautics and Astronautics, Stanford University

[2] Associate Professor and Chairman, Thermosciences Division, Department of Mechanical Engineering, Stanford University

$$T = \dot{m}\, v_e \qquad [1]$$

$$I_{sp} = v_e / g \qquad [2]$$

with the exhaust velocity, v_e, determined from the charge to mass ratio of the droplet (q/m), and the applied acceleration potential, ϕ:

$$v_e = \sqrt{2\,(q/m)\,\phi} \qquad [3]$$

Experimentally, the charge to mass ratio can be determined from the ratio of the beam emission current, I_b, and the mass flow rate:

$$q/m = \frac{I_b}{\dot{m}} \qquad [4]$$

The most-probable specific charge, q/m, is established by the Rayleigh criteria:

$$q/m \approx \frac{3\,(\varepsilon_o \gamma)^{1/2}}{\rho r^{3/2}} \qquad [5]$$

where ε_0 is the free space permittivity, γ is the surface tension of the propellant, ρ is the density of the propellant, and r is the radius of the particles. Determining (q/m) indirectly therefore requires a measurement of the beam current and mass flow rate (Eqn. 4) or of the particle radius. Below, we describe preliminary performance measurements using both methods, with the particle radius estimated by optical microscope examination of particles impacted onto a polished mirror.

B. On-Orbit Experiments

The EMERALD nanosatellite project is a two-spacecraft mission, joint between Stanford University and Santa Clara University, and funded through the Air Force Research Laboratory (AFRL) University Nanosatellite Program. Each of the 20 kg spacecraft is hexagonal in shape measuring 19” in diameter and 12” high. The spacecraft is scheduled for launch in 2002 on board the Space Shuttle. The CMT will be integrated into one of the EMERALD spacecraft [2,3]. The CMT on the 20-kg EMERALD nanosatellite is expected to have up to 8 m/s delta-velocity capability with 10 g of 2.0 M sodium-iodide seeded glycerol propellant, while consuming 6 Watts of maximum total system power.

An artist’s depiction of the spacecraft pair is shown in Figure 1.

To minimize experimental variables, the on-orbit firing of the CMT will involve simple operational testing monitored by proven methods. The thrust axis of the CMT will be offset from the center-of-gravity of the spacecraft so as to induce a spin. The Attitude Determination and Control System (ADCS) onboard the spacecraft will measure the spin by using light-sensors and the variation in the solar panel power output.

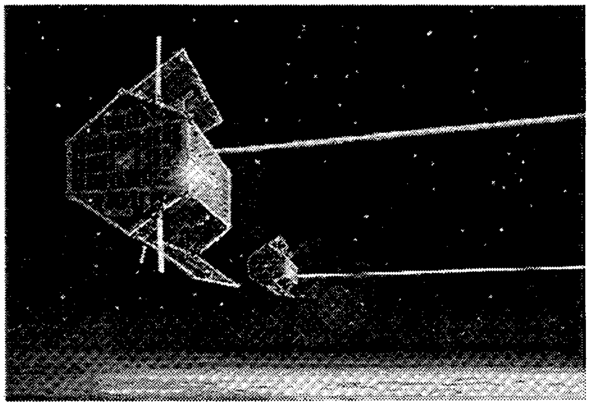

Figure 1. The EMERALD nanosatellite concept.

III. RESEARCH ACTIVITY

The research activities at Stanford University are focused primarily on the redevelopment, characterization, and miniaturization of the CMT technology. The culmination of the research effort is to flight qualify and test a CMT prototype for on-orbit propulsion. The redevelopment efforts make use of commercial-off-the-shelf miniature and micro technology, in some cases, redesigning these technologies for space application. Such an approach not only brings economic benefit but also allows for the rapid integration and deployment of the CMT technology.

IV. EXPERIMENTAL SETUP

A. CMT System Description

The CMT system contains a Thruster Control Unit (TCU), Propellant Storage and Delivery Unit (PSDU), and a Thruster Core (TCORE). The prototype CMT is shown in Figure 2. The block diagram of the CMT system is shown in Figure 3.

The TCU is based on the use of a PIC16F877 microcontroller and serves as the nerve center of the CMT package. The TCU accepts commands via I2C and RS232 serial communications, decodes the command, and then issues the appropriate analog and digital signals to control the rest of the CMT hardware. The TCU also collects telemetry and data from various sensors and transmits the data back to the spacecraft computer. The TCU contains custom software that allows for flexible operation of the CMT.

The PSDU is based on the use of a plunger mechanism driven by a DC-motor via a high ratio gearbox. The PSDU operation and the flow rate are controlled by the TCU. Latching control valves will prohibit premature propellant flow to the TCORE, and will be opened once the spacecraft is in orbit.

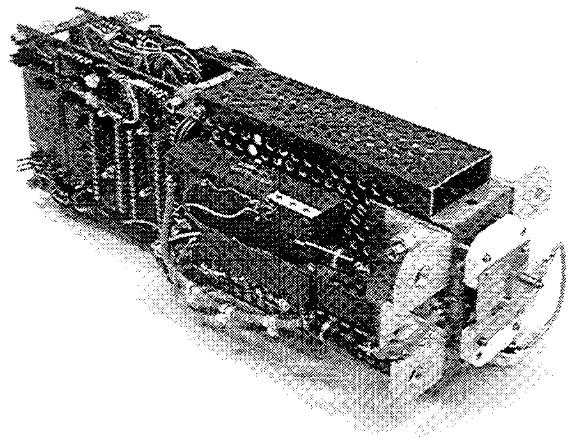

Figure 2. Photograph of the CMT prototype shown with a single-needle core.

Three different TCORE assemblies have been studied, but results are presented here, primarily for the single needle emitter core. The single-emitter core assembly has a 0.006 in OD / 0.002 in ID capillary stainless-steel emitter. A multi-emitter array core consisting of one hundred 0.006 in OD / 0.002 in ID capillary in a 10 by 10 array and a linear-slit geometry core with a 0.75 in by 0.003 in slit opening, built by Phrasor Scientific, Inc. of Duarte, CA, are also undergoing tests in our laboratory.

B. Vacuum Facility

The CMT experiments were conducted in a 4 in diameter Pyrex chamber. A chamber pressure of 10^{-7} Torr is sustained during firing by a Varian mechanical pump backed with an Alcatel CFF450 turbopump. The chamber pressure is monitored by a thermocouple vacuum gauge for course measurements, and an ionization gauge for high vacuum. Figure 4 shows a photograph of the CMT vacuum facility.

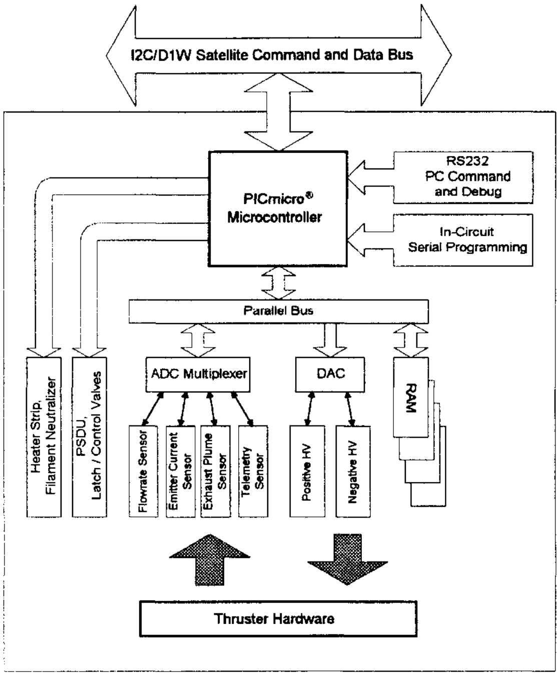

Figure 3. CMT operational block diagram.

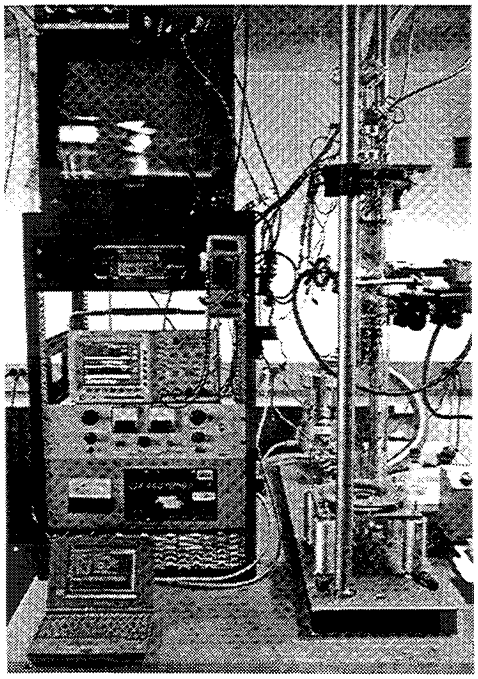

Figure 4. Photograph of the CMT test facility.

In all tests reported on here, the CMT was mounted facing upward (firing upward) in the chamber. The propellant was a solution consisting of 2.0 M sodium-iodide/glycerol. A Pentium/Windows 98 laptop handles all commands and data communication to the CMT by way of an RS232 connection via vacuum feedthroughs.

C. Indirect Measurement Experimental Setup

At present, the facility allows for an indirect measurement of the performance, which was implemented for nominal firing conditions using the single-emitter core. The measurement uses the emission current and acceleration voltage to calculate the thrust and specific impulse. A second method, based on a time-of-flight measurement, monitors the emission current decay over time immediately following a termination in the acceleration potential. The time-of-flight hardware has been integrated into the experiment, but preliminary measurements have not yet been analyzed.

A collector plate is used to capture the emission current from the CMT. A grounded cage surrounds the collector plate, forming a Faraday cage to help shield the collector from external noise. The collector plate and Faraday cage can be seen in the photograph in Figure 5. In this photograph, the thruster (not shown) fires through the rectangular aperture, and the collector is at about a 45° angle to the cluster ion beam. The detector plate is coated with Aquadag® to minimize the perturbation on the beam current due to the secondary electron emission from the collector.

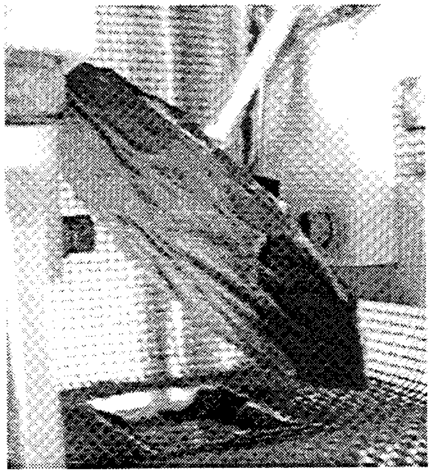

Figure 5. Close-up photograph of the detector plate housed within a Faraday cage.

For monitoring the beam current, the collector plate is connected to a Keithley 487 picoammeter. A Tektronix TDS3014 oscilloscope records the resulting voltage output from the picoammeter. In the time-of-flight measurement (results not reported on here), a Keithley 417 high-speed current amplifier connected to the collector plate monitors the beam emission current decay. A Tektronix TDS3014 oscilloscope records the resulting voltage output from the current amplifier. The switching off of the acceleration potential is accomplished by connecting the CMT source plate to ground by way of a high-voltage reed relay.

Where possible, the mass flow rate is calculated by three independent methods. The first method obtains the time-averaged mass flow rate by dividing the mass of the propellant deposited onto the collector by the thruster operation time. This method requires operation over extended duration, to achieve a measurable amount of change in the collector weight. The second method obtains the mass flow rate by measuring the displacement of the meniscus in the propellant line. The third method obtains the mass flow rate directly from the PSDU calibration.

V. RESULTS

A. I-V Curve

The measurement of time-averaged beam emission current as a function of acceleration potential is presented in Figure 6. In general, the thruster beam current is found to increase exponentially with the voltage applied between the source needle, and the extractor (acceleration voltage). While the time-averaged beam current ranged from 0.1 to 1 μA, burst with up to 15 μA were detected at acceleration potentials of around 5.5-6.0 kV.

B. Performance Parameters

The thrust and specific impulse was determined indirectly through Eqns. 1-5 above. The results are shown in Figure 7 and Figure 8, respectively. As expected, we see an increase in thrust with increased acceleration potential, varying from about 1μN at a potential of 2.6 kV, to 5 μN at a potential of 4.4 kV. A similar trend is seen in the specific impulse, ranging from approximately 60 sec at 2.6 kV, to 200 sec at 4.4 kV. While these values are relatively low for electric rocket technologies, we believe that improved control of propellant flow for potentials

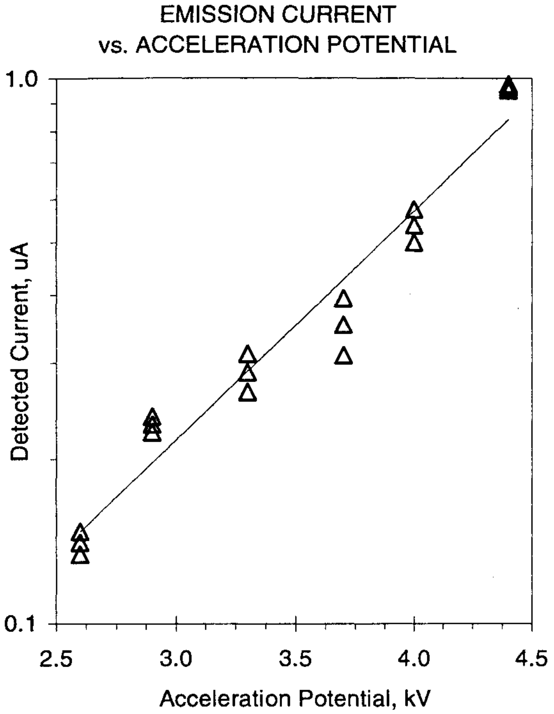

Figure 6. Single-needle beam emission current as a function of acceleration potential.

beyond 5 kV can lead to a specific impulse in excess of 400 sec, which is certainly acceptable for a first prototype of this type of rocket. The intermittent 15 μA current bursts which persisted beyond 4.4 kV in acceleration potential resulted in estimated bursts in thrust of approximately 35μN, and in specific impulse of about 600 sec, at 6 kV.

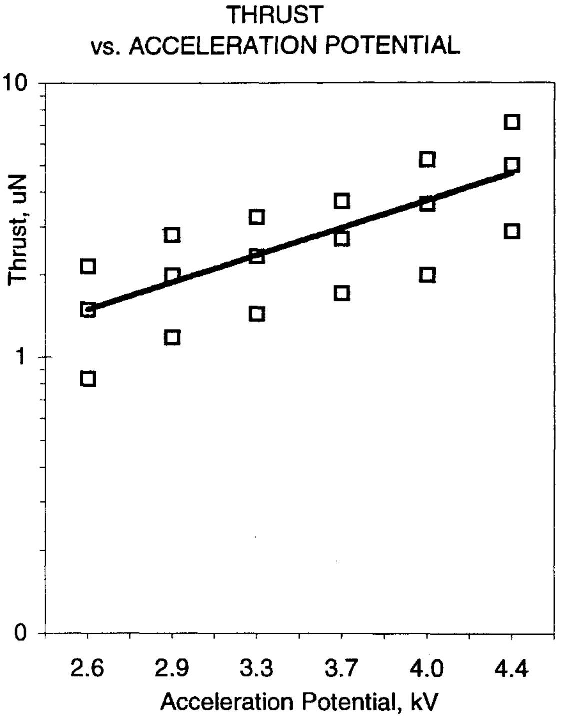

Figure 7. Single-needle core thrust as a function of acceleration potential..

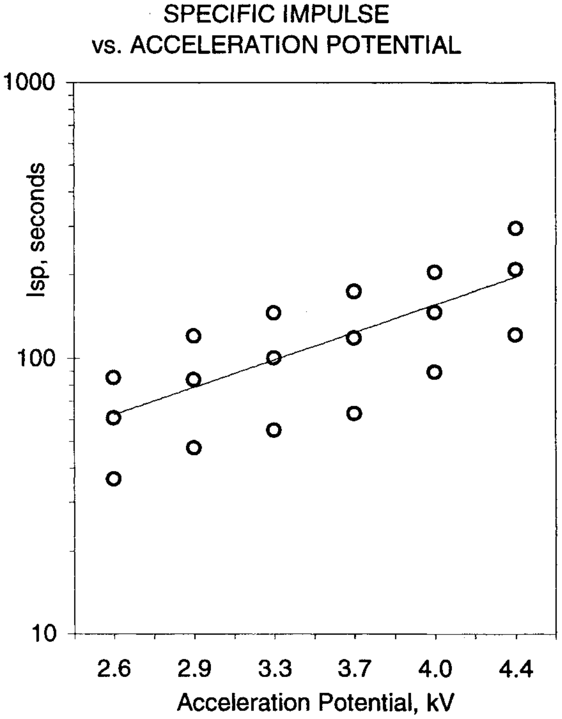

Figure 8. Single- Single-needle core specific impulse as a function of acceleration potential.

C. Efficiency

While the efficiency of the electrohydrodynamic process itself is expected to be high, also of interest is the *overall system efficiency*, η_{SYSTEM}, which is defined as the ratio of the thruster beam power, $P_{emission}$, to the total system dissipated power, P_{system}, i.e.,

$$\eta_{SYSTEM} = \frac{P_{emission}}{P_{system}} \qquad [6]$$

Here, P_{system} is includes the power consumption of the microcontroller, its supporting curcuitry, the PSDU, as well as the power losses through the high-voltage power supplies. The system efficiency is affected by numerous factors, but is determined primarily by the efficiency of the high-voltage power supplies and the design of the thruster core.

The CMT *core power efficiency*, η_{TCORE}, can be defined as follows:

$$\eta_{TCORE} = \frac{P_{emission}}{P_{emission} + P_{loss}} \qquad [7]$$

where

$$P_{emission} = \phi \cdot I_b \qquad [8]$$

is the emission power as detected by the beam current at the collector, and and where

$$P_{loss} = \phi \cdot I_{loss} \qquad [9]$$

with the current loss I_{loss} is defined as:

$$I_{loss} = I_{core} - I_b \qquad [10]$$

i.e., the difference between the total current delivered to the thruster core, and that which is actually translated into charged particle beam current, I_b.

Experimental results for η_{TCORE} is shown in Figure 9. The core efficiency for a single-needle emitter is seen to vary between 20% and 40%. Losses are found to be primarily due to current leakage across the dielectric insulator separating the needle base and the extractor. It is noteworthy that with a thruster core design that employs multiple emitter or emission sites, $P_{emission}$ will be multiplied by the number of emitters or emission sites, while $P_{leakage}$ is expected to remain constant. For a 100 emitter needle array, extrapolating the results for the single-needle core efficiency, the efficiency is expected to be in excess of 90%. The core power efficiency will increase as the number of emitters or emission sites is increased, and if the leakage current across the insulator does not change.

VI. SUMMARY AND FURTHER DISCUSSION

The Colloid micro-thruster prototype has operated for more than 100 hours in 10^{-7} Torr vacuum with repeated cold and warm starts. Nominal thrust levels of 0.5-4.0 micronewton per needle with up to 200 seconds of specific impulse have been recorded and regularly reproduced. However thrust levels up to 35 micronewton per nozzle at higher than 600 seconds specific impulse, corresponding to operation at higher acceleration potential, has been recorded, resulting from intermittent bursts of emission at potentials in excess of 4.4 kV.

Thruster core power efficiency of the single-needle thruster core reported on here reaches up to 40%, and is expected to go as high as 90% for the

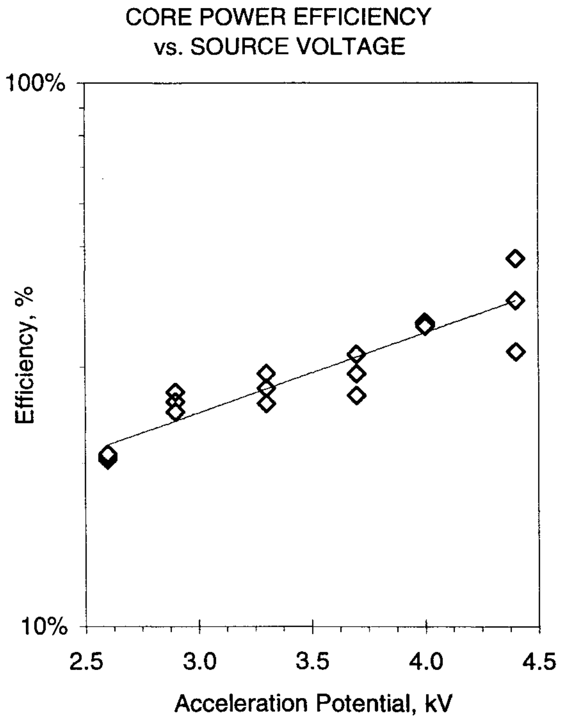

Figure 9. Single-needle thruster core power efficiency, as defined by Eqn. 7.

100-nozzle capillary array thruster core. The importance of a good thruster core design and its effect on the overall system efficiency and reliability cannot be overemphasized. Experiments involving the single-nozzle thruster core with a guide electrode, shown in Figure 10, showed significant performance improvement by reducing deposits on the extractor plate, as shown in Figure 11. The guide electrode serves to better shape the electric field between the source needle and the extractor. It is maintained at the same potential as the source needle, and in our core design, can be adjusted in position so as to achieve an optimum field distribution.

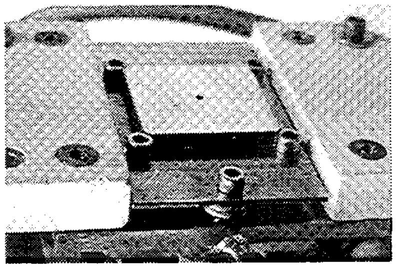

Figure 10. Guide-electrode over the source plate on the single-nozzle thruster core.

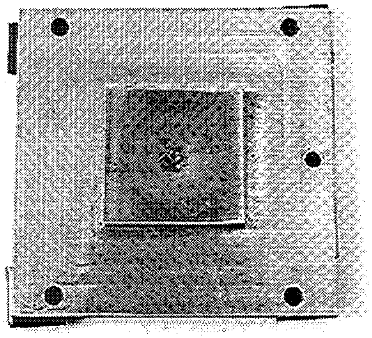

Figure 11. Propellant deposit on extractor plate, operated for extended duration without a guide electrode.

Development Challenges

The development effort of the colloid micro-thruster prototype faces a number of unique challenges. The goal to build a flight-qualified thruster, as oppose to a laboratory unit, favors the design to take an integrated system approach, with the resulting design directly applicable to commercial CMT.

The integrated system approach in the design of the CMT also resulted in a much simpler design. This plays a significant role in the qualification of the CMT for flight on board the Space Shuttle. The CMT design has passed the first of three Safety Reviews by the Space Shuttle Payload Safety Review Panel, and is moving forward toward full flight certification.

One of most difficult challenge is to achieve a reliable, extended operation with combined cold and warm starts. The reliable extended operation that has been achieved for the single-needle thruster core, is difficult to achieve with the capillary array thruster core. With the capillary array thruster core, the alignment between the capillary and the extractor openings are critical. This is dictated by manufacturing methods and precision. Even slight misalignment is enough to affect the field lines so as to cause the emitted particle trajectories to deviate and strike the extractor. Extractor strikes reduces the overall system efficiency. Furthermore, extended extractor strikes will lead to propellant accumulation and eventually results in the shorting of the acceleration potential and system shutdown.

VII. ACKNOWLEDGMENT

The colloid micro-thruster research project is sponsored by the Air Force as a subcontract on a Phase II STTR project through Phrasor Scientific. The authors also wish to thank Phrasor Scientific, Inc., the University Nanosatellite Program and the Nanosatellite support team from AFRL, NASA GSFC and NASA JSC, for their guidance on this research activity. Finally, the authors wish to thank the Stanford University's Space Systems Development Laboratory, in particular the EMERALD Nanosatellite Team for their support.

VIII. REFERENCES

[1] Mueller, J., AIAA 97-3058, 33rd Joint Propulsion Conference, Seattle, WA, July 1997.

[2] Kitts, Christopher A., Robert J. Twiggs, Jonathan How, Freddy Pranajaya, and Bryan Palmintier, "Emerald: A Low Cost Formation Flying Technology Validation Mission", In Proceedings of the 1999 IEEE Aerospace Conference, Snowmass, CO, March 6-13, 1999.

[3] Kitts, Christopher A., Freddy Pranajaya, Julie Townsend, and Robert J. Twiggs, "Emerald: An Experimental Mission in Robust Distributed

Space Systems", In Proceedings of the 13th Annual AIAA/USU Conference on Small Satellites, Logan, Utah, August 23-26, 1999.

[4] Pranajaya, F., "Progress on Colloid Micro-Thruster Research and Flight Testing", In Proceedings of the 13th Annual AIAA/USU Conference on Small Satellites, Logan, Utah, August 23-26, 1999.